Preprint typeset in JHEP style - HYPER VERSION

Fast and Slow Coherent Cascades in Anti-de Sitter Spacetime

Fotios V. Dimitrakopoulos[*], **Ben Freivogel**[†] **and Juan F. Pedraza**[‡]

GRAPPA and ITFA, Institute of Physics, Universiteit van Amsterdam, Science Park 904, 1090 GL Amsterdam, Netherlands

Abstract: We study the phase and amplitude dynamics of small perturbations in 3+1 dimensional Anti-de Sitter spacetime using the truncated resonant approximation, also known as the Two Time Framework (TTF). We analyse the phase spectrum for different classes of initial data and find that higher frequency modes turn on with coherently aligned phases. Combining numerical and analytical results, we conjecture that there is a class of initial conditions that collapse in *infinite slow time* and to which the well-studied case of the two–mode, equal energy initial data belongs. We additionally study perturbations that collapse in finite time, and find that the energy spectrum approaches a power law, with the energy per mode scaling approximately as the inverse first power of the frequency.

arXiv:1612.04758v1 [hep-th] 14 Dec 2016

[*]f.dimitrakopoulos@uva.nl

[†]benfreivogel@gmail.com

[‡]jpedraza@uva.nl

Contents

1. Introduction **1**

2. Spherically Symmetric Perturbations in AdS. **3**

2.1 Phase-coherent power laws 6

3. The two–mode data **7**

3.1 Numerical results 7

3.2 A speed limit for energy transfer 11

4. Gaussian Data **13**

5. Conclusion **16**

1. Introduction

The question of stability of global Anti-de Sitter spacetime under small perturbations was energized by the seminal work of P. Bizon and A. Rostworowski [1], in which they traced the evolution of small perturbations in the form of a spherically symmetric scalar field. For most of the field profiles they studied, they found that the perturbation would eventually collapse to a black hole and the time of the collapse scales as the inverse square power of the amplitude ϵ of the perturbation. However, subsequent work on the subject has revealed a very rich and intriguing dynamics of the problem [2–30].

Many initial data were found that do not collapse [6–12] and at the same time analytic studies [3,4] suggested that non-collapsing solutions survive in the small amplitude limit. Numerical results are limited to finite–energy perturbations, while it is interesting one to address the zero–energy limit. Perturbation theory [4, 13, 16] has proven to be quite fruitful in this direction. The resulting system of equations possesses a scaling symmetry which allows us to draw conclusions about the small amplitude ($\epsilon \to 0$) limit from results obtained at finite ϵ. This scaling symmetry can be used to show that 'stability islands' persist in the small amplitude limit.[1]

[1]Due to this result, these areas of stability are not actually *islands* since they are connected to each other through empty AdS [3].

In momentum space, the evolution of the perturbation towards a black hole translates to an efficient transfer of energy to modes with higher frequencies. Due to the fact that the frequencies linearized modes of AdS are commensurate, efficient energy transfer occurs and conventional perturbation theory breaks down. There are modifications of the perturbation theory that can effectively capture the transfer of energy between different modes up to the first nonlinear timescale $t \sim \epsilon^{-2}$, known by the names: *two time scale formalism* (TTF) [13], *renormalization group perturbation method* [16, 17] or *resonant approximation* [31]. All of these techniques capture the effect of efficient energy transfer through a *slow time* dependence of the amplitudes and the phases of the linearized modes.

In this paper we study the evolution of the phases and the amplitudes of the Fourier modes, in the Two Time Framework (TTF) approximation, for a variety of initial conditions, and we find that the phases are not excited in a random way, as in the standard theory of weak turbulence, but in a quite coherent way, supporting the coherent phase ansatz of [5]. However, we observe small deviations from a strictly coherent phase spectrum, suggesting that the conjecture [5] should be refined.

We study the evolution of the two-mode, equal energy initial data, and we provide a combination of numerical and analytic evidence to support the conjecture that they belong to a class of initial conditions that collapse in **infinite slow time**[2]. We show analytically that solutions dominated by the two lowest modes obey a simple speed limit on the rate of energy transfer to higher frequencies. The speed limit depends on the frequency; we show that in $3+1$ dimensions it takes infinite time to transfer energy to arbitrarily high frequency, while in higher dimensions it takes finite time.

A nice way to track energy transfer in this system is the so-called *analyticity strip method* [31–33], which diagnoses at what time the amplitude spectrum ceases to decrease exponentially at large mode numbers. We find numerically that, for the two-mode initial data, the width of the analyticity strip goes to zero **exponentially** in time. There has been a long-lasting dispute about the ultimate fate of this initial data [9, 13, 34] and we hope we settle the issue with this work.[3]

We also study initial data that has a Gaussian profile. We find that this data collapses in finite slow time. In addition, we find that at the time of the collapse the amplitudes A_n of the normal modes approach a power-law spectrum of the form

[2]At the vanishing amplitude limit, $\epsilon \to 0$.

[3]The fact that this data might collapse in infinite slow time was suggested earlier to us by Andrzej Rostworowski, as we understand, based on simulations of full General Relativity in AdS. It is our understanding that A. Rostworowski and collaborators have also obtained interesting results about this $3+1$-dimensional problem, and we look forward to comparing them to our results.

$A_n \sim n^{-\gamma}$ with $\gamma \approx 3/2$, which modifies slightly the result $\gamma = 8/5$ reported in [35].[4] This amplitude spectrum corresponds to an energy spectrum $E_n \sim 1/\omega_n$.

In Sec.(2) we review the model of spherically symmetric scalar perturbations in AdS and the perturbation theory leading to the Two Time Framework (TTF). In Sec.(3) we study both numerically and analytically the case of the two-mode equal energy data, while in Sec.(4) we present numerical results about the evolution of *narrow* Gaussian wavepackets.

2. Spherically Symmetric Perturbations in AdS.

For completeness, we will review in this section the model of spherically symmetric, scalar field perturbations of [1] as well as the TTF system [13,16] and the *phase coherent* conjecture of [5].

We consider a self gravitating, spherically symmetric scalar field ϕ in asymptotically AdS_4. The corresponding metric is of the form

$$ds^2 = \frac{1}{\cos^2 x}\left(-Ae^{-2\delta}dt^2 + A^{-1}dx^2 + \sin^2 x d\Omega^2\right), \tag{2.1}$$

where, for simplicity, we have set the AdS radius to 1. Due to spherical symmetry A, δ and ϕ are only functions of time t and the radial coordinate $x \in [0, \frac{\pi}{2})$. It is customary to introduce the auxiliary variables $\Phi = \phi'$ and $\Pi = A^{-1}e^{\delta}\dot{\phi}$ with the use of which the equation of motion for ϕ can be written as:

$$\dot{\Phi} = \left(Ae^{-\delta}\Pi\right)', \qquad \dot{\Pi} = \frac{1}{\tan^x}\left(\tan^2 x Ae^{-\delta}\Phi\right)', \tag{2.2}$$

while the Einstein equations reduce to the constraints:

$$\begin{aligned} A' &= \frac{1+2\sin^2 x}{\sin x \cos x}(1-A) - \sin x \cos x A\left(\Phi^2+\Pi^2\right) \\ \delta' &= -\sin x \cos x\left(\Phi^2+\Pi^2\right). \end{aligned} \tag{2.3}$$

The overdots and the primes here denote differentiation with respect to t and x respectively, and the pure AdS solution is given by $\phi = 0$, $A = 1$ and $\delta = 0$. One can try and solve this system analytically in perturbation theory, expanding the fields in powers of the amplitude ϵ of the initial perturbation

$$\phi = \sum_{j=0}^{\infty} \epsilon^{2j+1}\phi_{2j+1}(t,x), \quad A = 1 - \sum_{j=0}^{\infty}\epsilon^{2j}A_{2j}(t,x), \quad \delta = \sum_{j=0}^{\infty}\epsilon^{2j}\delta_{2j}(t,x). \tag{2.4}$$

[4] The fact that the exponent might be smaller than 8/5 was also conveyed to us in a discussion with A. Rostworowski and collaborators.

Inserting this ansatz into the equations of motion and collecting terms of the same order of ϵ we obtain a set of linear equations which can be solved order by order. To first order, we merely have a scalar filed propagating in the AdS background

$$\ddot{\phi}_1 + L\phi_1 = 0. \tag{2.5}$$

Here, $L = -\frac{1}{\tan^2 x}\partial_x \left(\tan^2 x \partial_x\right)$ is the Laplacian of AdS with eigenvalues $\omega_j = (2j+3)$ and eigenfunctions

$$e_j = d_j \cos^3 x_2 F_1\left(-j, 3+j, 3/2; \sin^2 x\right), \qquad d_j = \sqrt{\frac{16}{\pi}(j+1)(j+2)}. \tag{2.6}$$

The eigenfunctions are normalized such that $(e_m, e_n) = \delta_{mn}$ in the inner product $(f,g) := \int_0^{2\pi} f(x), g(x) \tan^2 x dx$ and the positivity of the eigenvalues implies that AdS is linearly stable. One can use the eigenfunctions of L to expand the field ϕ, where at this order is simply:

$$\phi_1(t,x) = \sum_{j=0}^{\infty} c_j^{(1)}(t) e_j(x) = \sum_{j=0}^{\infty} \left(\alpha_j e^{i\omega_j t} + \bar{\alpha}_j e^{-i\omega_j t}\right) e_j(x). \tag{2.7}$$

To second order in ϵ we obtain the back reaction on the metric

$$A_2(t,x) = -\nu(x) \int_0^x \left(\dot{\phi}_1(t,y)^2 + \phi'(t,y)^2\right) \mu(y) dy, \tag{2.8}$$

$$\delta_2(t,x) = \begin{cases} -\int_0^x \left(\dot{\phi}_1(t,y)^2 + \phi'(t,y)^2\right) \nu(y)\mu(y) dy, & \text{for } \delta(t,0) = 0 \\ \int_x^{\pi/2} \left(\dot{\phi}_1(t,y)^2 + \phi'(t,y)^2\right) \nu(y)\mu(y) dy, & \text{for } \delta(t,\pi/2) = 0. \end{cases} \tag{2.9}$$

while the first non–trivial dynamics appear at the third order. One obtains the inhomogeneous equation

$$\ddot{\phi}_3 + L\phi_3 = S\left(\phi_1, A_2, \delta_2\right), \tag{2.10}$$

where $S = -2\ddot{\phi}_1 \left(A_2 + \delta_2\right) - \dot{\phi}_1 \left(\dot{A}_2 + \dot{\delta}_2\right) - \phi_1' \left(A_2' + \delta_2'\right)$. We can again expand the field as $\phi_3(t,x) = \sum_{j=0}^{\infty} c_j^{(3)}(t) e_j(x)$, and projecting o the basis $\{e_m\}$, we obtain an infinite set of decoupled forced harmonic oscillators for the Fourier coefficients

$$\ddot{c}_j^{(3)}(t) + \omega_j^2 c_j^{(3)}(t) = S_j, \quad S_j \equiv (S, e_j). \tag{2.11}$$

Due to the fact that the linear spectrum is highly commensurate, since the frequencies are integers, there can be many resonant terms contained in S_j. Specifically, for every

triad (j_1, j_2, j_3)[5] such that $\omega_j = \omega_{j_1} + \omega_{j_2} - \omega_{j_3}$ there is a resonant term in S_j. A first treatment of these resonances appeared in [1] but a more sophisticated technique, the Two Time Framework [13, 16], was later developed and allows for a systematic treatment. The basic idea behind TTF, is to allow for an additional, *slow time* dependence, of the fields. In that case, the perturbative expansion of the fields, would become

$$\begin{aligned} \phi &= \epsilon\phi_1(t,\tau,x) + \epsilon^3\phi_3(t,\tau,x) + \mathcal{O}(\epsilon^5), \\ A &= 1 - \epsilon^2 A_2(t,\tau,x) + \mathcal{O}(\epsilon^4), \\ \delta_2 &= \epsilon^2\delta_2(t,\tau,x) + \mathcal{O}(\epsilon^4), \end{aligned} \tag{2.12}$$

where $\tau = \epsilon^2$ denotes the slow time. One could go to higher orders by introducing additional slow time variables. Substituting now the above expansion, eq. (2.12), into the equations of motion, eq. (2.2)-(2.3), we obtain again a system of equations which can be solved order by order in ϵ. The difference now, is that the expansion for the *linearized* field can be written as

$$\phi_1(t,\tau,x) = \sum_{j=0}^{\infty} \left(\alpha_j(\tau)e^{-i\omega_j t} + \bar{\alpha}_j(\tau)e^{-i\omega_j t}\right) e_j(x), \tag{2.13}$$

where the slow time τ accounts for the energy transfer among the normal modes (due to non–linearities), while the fast time t accounts for the oscillations of the normal modes. To second order we have again the constraints for A_2 and δ_2 and the first non-trivial dynamics appear to third order in ϵ

$$\partial_t\phi_3 + L\phi_3 + 2\partial_t\partial_\tau\phi_1 = S(\phi_1, A_2, \delta_2), \tag{2.14}$$

where the source term reads $S(\phi_1, A_2, \delta_2) = (\dot{A}_2 - \dot{\delta}_2)\dot{\phi}_1 - 2(A_2 - \delta_2)L\phi_1 + (A_2' - \delta_2')\phi_1'$. The overdots here, represent derivatives with respect to the fast time t, as usual. Projecting again on the basis $\{e_m\}$, and substituting eq. (2.13) we obtain

$$\left(e_j, \partial_t^2\phi_3 + \omega_j^2\phi_3\right) - 2i\omega_j\left(\partial_\tau\alpha_j(\tau)e^{-i\omega_j t} - \partial_\tau\bar{\alpha}_j(\tau)e^{i\omega_j t}\right) = (e_j, S)\,. \tag{2.15}$$

Now we can treat the resonances separately, due to the presence of terms proportional to $e^{\pm i\omega_j t}$ on the left hand side. Setting

$$-2i\omega_j\partial_\tau\alpha_j(\tau) = (e_j, S)\,[\omega_j] = \sum_{klm} S_{jklm}\bar{\alpha}_k\alpha_l\alpha_m, \tag{2.16}$$

we may cancel off the resonant terms from the rest of the eq. (2.14). These are now entirely captured by eq. (2.16), rendering the solution ϕ_3 bounded, and hence of little

[5] S_j is cubic in a_j at this order.

interest to us. The result is an infinite set of coupled first order ODEs for the Fourier coefficients of the linear expansion, which are known by the name TTF *equations*. The sum, in eq. (2.16), contains only terms for which the *resonance condition* $j+k=l+m$ is satisfied.[6] The TTF equations govern the evolution of both the amplitudes and the phases of the complex coefficients a_j and hence, a perhaps more convenient way to rewrite them, is by going to the *amplitude–phase representation* $\alpha_j(\tau) = A_j(\tau)e^{iB_j(\tau)}$, in terms of which the TTF equations can be expressed as

$$2\omega_j \frac{dA_j}{d\tau} = \sum_{\substack{j+k=l+m \\ j\neq l, j\neq m}} S_{jklm} A_k A_l A_m \sin\left(B_j + B_k - B_l - B_m\right) \tag{2.17}$$

$$2\omega_j \frac{dB_j}{d\tau} = T_j A_j^2 + \sum_{i\neq j} R_{ij} A_i^2 + A_j^{-1} \sum_{\substack{j+k=l+m \\ j\neq l, j\neq m}} S_{jklm} A_k A_l A_m \cos\left(B_j + B_k - B_l - B_m\right). \tag{2.18}$$

Here $T_j = S_{jjjj}$, $R_{ji} = S_{ijji} + S_{jiji}$, for $i \neq j$. This system of equations possesses the important scaling symmetry, $\alpha_j(\tau) \to \epsilon\alpha_j(\tau/\epsilon^2)$, which means that the evolution of a perturbation of amplitude A_j for time τ, will be the same as the evolution of the perturbation of amplitude ϵA_j, but for longer time τ/ϵ^2. As mentioned earlier, this allows us, for as long as the TTF approximations are valid [3], to draw conclusions for the vanishing amplitude limit, from results obtained in finite ϵ.

2.1 Phase-coherent power laws

In [5] it was suggested that a power-law spectrum alone might not be sufficient for a black hole to form, but the phases need to be coherent as well. In this context the coherence of the phases is defined as a phase spectrum that is *asymptotically* linear in the mode number n

$$B_n(\tau) = \gamma(\tau)n + \delta(\tau) + \ldots, \tag{2.19}$$

where the ellipsis represent subleading terms. part of this work is to quantify the degree of coherence of the phases for different initial data, and look for possible deviations. In addition, as it was already argued in [5], the case of AdS_{3+1} is subtle and a numerical study of the evolution of the phases, using the actual interaction coefficients S_{ijkl}, and not just their asymptotic values, is of importance.

[6] In principle, all the resonant *channels*, $j = \pm k \pm j \pm l$, should appear but only the one described here remains [16, 24].

3. The two–mode data

We will start by looking at two mode–initial data, which is parametrized as follows:

$$A_n = \frac{\epsilon}{3}\left(\delta_n^0 + \kappa\delta_n^1\right). \tag{3.1}$$

This is the case where we initially excite the lowest two modes with no relative phase. Here, ϵ denotes the amplitude of the perturbation, while κ parametrizes the amount of energy in the second lowest mode. For concreteness, we have considered data with $\epsilon = 1$ and different values of κ. However, as discussed before, the TTF equations are invariant under the scaling symmetry $\alpha_n(\tau) \to \epsilon\alpha_n(\tau/\epsilon^2)$. Therefore, the solution for different values of ϵ would be completely equivalent to the case $\epsilon = 1$ but evolved to a different time $\tau_{\rm max}$.

3.1 Numerical results

Equal energy:

Setting $\kappa = 3/5$ corresponds to a situation where the energy is equally distributed between the two modes. This case is very interesting since it has been argued to be in the borderline of one of the stability islands [9, 13, 34]. Here, instead of looking at the value of Π at the origin,[7] we would like to concentrate on the spectrum of the amplitudes and the phases, hoping to shed some light from a different perspective and clarify the fate of this initial condition.

In order to detect the formation of singularities from the spectrum we use the so-called analyticity strip method, introduced in [32], and employed for the first time in the context of the AdS instability problem in [33]. The idea here is to consider the the analytic extension of $\phi(t, z)$ into the complex plane of the radial variable $r \to z \in \mathbb{C}$. The function $\phi(t, z)$ will typically have complex singularities moving in time; if one of these singularities hits the real axis, $\phi(t, r)$ becomes singular. The pair of singularities closest to the real axis are denoted as $z = x \pm i\rho$, so that ρ determines the width of the analyticity strip around the real axis. Thus, if ρ vanishes at some point during the evolution then $\phi(t, r)$ will be singular. Now, ρ is encoded in the exponential decay of the fourier coefficients $A_n \sim e^{-\rho n}$ (at large n), so it can be obtained from the asymptotics of a given numerical solution.

In order to evolve the system of equations (2.17)-(2.18) we need to fix the gauge and find the coefficients S_{ijkl} up to a maximum number $i = j = k = l = n_{\rm max}$. We

[7] The value of $\Pi(t, 0)$ at the origin corresponds to the Ricci scalar and therefore is a good indicator of singularity.

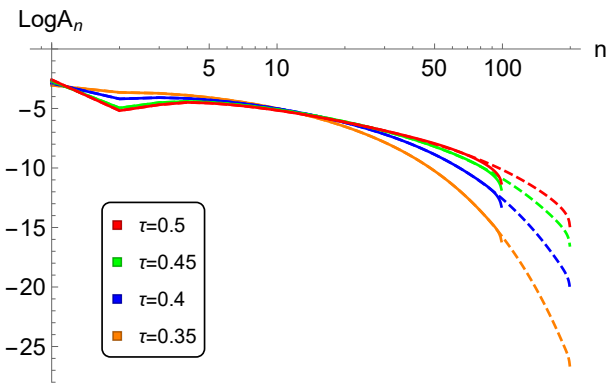

Figure 1: Amplitude spectrum A_n, for different values of τ. Solid lines correspond to a 100 mode truncation, while dashed lines correspond to a 200 mode truncation.

choose to work in the boundary gauge, where $\delta(t, \pi/2) = 0$, since in this gauge the evolution of the phases is regular [2, 15, 21] (and therefore, the numerical integration is easier). In order to estimate the effect of the cutoff $n_{\max}$ we evolve the system for two different cases, first for $n_{\max} = 99$ and then for $n_{\max} = 199$. In Fig. (1) we show the amplitude spectrum in the two cases, for different values of τ. In general they agree over a wide range of n, but differ mildly in the range $n \in (79, 99)$. Next, we fit the amplitudes using the following ansatz

$$A_n(\tau) \sim \alpha(\tau) n^{-\gamma(\tau)} e^{-\rho(\tau) n} \,. \tag{3.2}$$

We exclude the modes $n \in (70, 99)$ for $n_{\max} = 99$ and $n \in (140, 199)$ for $n_{\max} = 199$ to avoid any cutoff effect. Also, since the analyticity strip method applies only asymptotically, we also exclude the first modes, $n \in (0, 29)$ for $n_{\max} = 99$ and $n \in (0, 59)$ for $n_{\max} = 199$. Comparing the two fittings should then provide a good test of our numerics, since the two ranges of n barely intersect with each other.

In Fig. (2) we plot the evolution of ρ and its derivative as a function of τ for the two cases considered, $n_{\max} = 99$ and $n_{\max} = 199$. In general, they are in excellent agreement for the first part of the evolution, but eventually they start to differ. Since ρ is the most robust parameter in the fitting (since it appears in the exponential), we define $\tau_{\max} \sim 0.485$ as the maximum time such that $|\rho_{199} - \rho_{99}| \leq 1/n_{\max}$; beyond this point the two ρ start to differ subtantially and we cannot trust our numerical evolution. We see that up to $\tau_{\max} \sim 0.485$, ρ decays almost exponentially, so we fit it as

$$\rho(\tau) \sim \rho_0 e^{-\alpha\tau} + \rho_\infty \,. \tag{3.3}$$

Interestingly, we find that $\rho_\infty \sim 5 \times 10^{-5} \ll 1/n_{\max}$ strongly supporting the idea that $\rho \to 0$ at infinite τ! The value of γ varies very little before $\tau_{\max}$ —see Fig. (3)— but

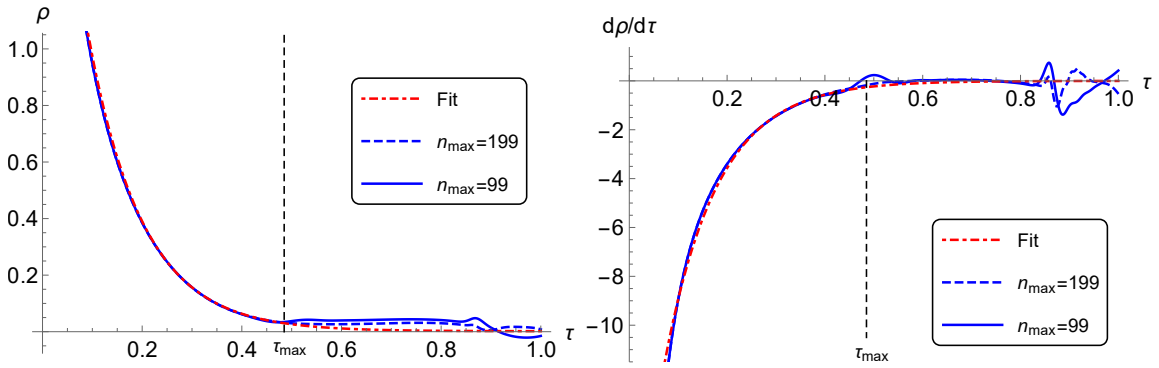

Figure 2: Left: Evolution of $\rho(\tau)$ for $n_{\max} = 99$ and $n_{\max} = 199$. We define $\tau_{\max} \sim 0.485$ as the maximum time such that $|\rho_{199} - \rho_{99}| \leq 1/n_{\max}$; beyond this point we do not trust our numerical evolution. We have also included the best fit up to this time, using the ansatz $\rho(\tau) = \rho_0 e^{-\alpha\tau} + \rho_\infty$. This yields $\rho_\infty \sim 5 \times 10^{-5} \ll 1/n_{\max}$ which strongly supports the idea that $\rho \to 0$ as $\tau \to \infty$. **Right:** Evolution of $d\rho/d\tau$ for $n_{\max} = 99$ and $n_{\max} = 199$. The behavior of the derivative for $\tau < \tau_{\max}$ shows that the exponential function is indeed a good fit for ρ.

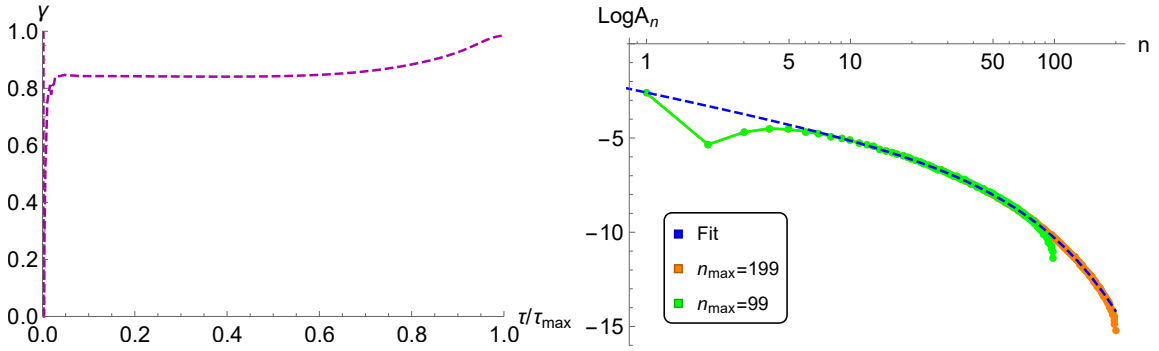

Figure 3: Left: Evolution of $\gamma(\tau)$ up to $\tau_{\max} \sim 0.485$. Beyond this point $\gamma(\tau)$ behaves quite erratically, also indicating the breakdown of our numerical solution. It seems difficult to extrapolate γ for $\tau \to \infty$. **Right:** Fitting of the amplitud spectum at $\tau = \tau_{\max} \sim 0.485$ according to the formula (3.2).

fluctuates quite a lot after this time. This makes it imposible to extrapolate its value to $\tau \to \infty$. We also plot the fiting function (3.2) at $\tau = \tau_{\max}$, finding an excellent agreement even outside of the range of n that we considered for the fits. This suggests that the formula (3.2) is actually quite robust, at least for the times at which we can trust our numerical results, $\tau \leq \tau_{\max}$.

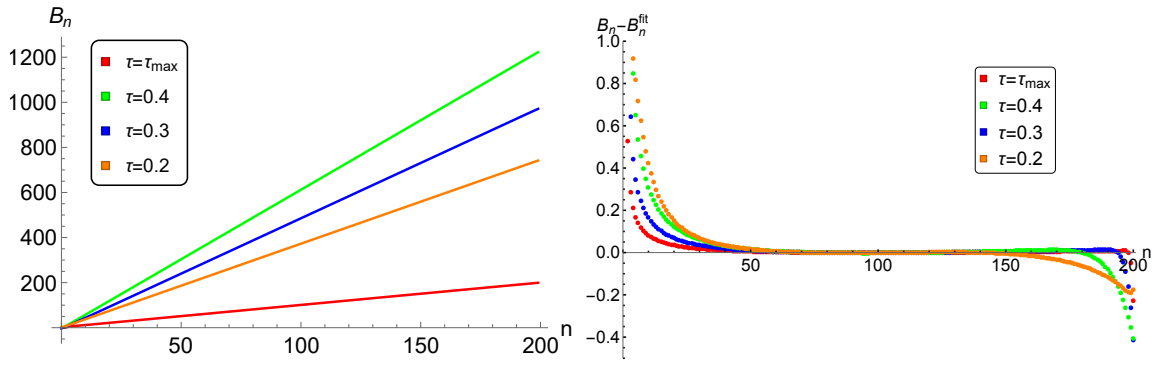

Figure 4: Left: Unwrapped phases B_n as a function of n for various values of τ. In all cases we see that the phases are perfectly aligned to form a straight line as in (2.19). **Right:** The difference between the fitted and the actual values as a function of n.

It is also interesting to put to test the validity of the phase coherent conjecture [5], which states that the asymptotic spectrum of phases align coherently as in (2.19). In order to see if this is actually true, we plot in Fig. (4) B_n as a function of n for various values of τ.[8] Interestingly, we see an almost perfect line for $\tau \leq \tau_{\max}$, with deviations from linearity being indistinguishable to the naked eye. To quantify the linearity of the spectrum we subtract the fitted values from the actual data. The results are presented in Fig. (4) as well. We observe a very good agreement with the linear, especially in the range of values used for the fit, $60 \leq n < 140$.

Non-equal energy:

For other values of κ, (3.1) implies that the initial energy of the two modes is different. We evolved the system for a wide range of κ and repeated the analysis that we presented for the case $\kappa = 3/5$. In extreme cases where most of the energy is deposited in one of the modes, the system can be though of a perturbation of a single mode solution, which is actually the center of one of the stability islands for AdS perturbations [3, 7, 36]. In such cases we do not expect black hole formation. On the other hand, values of κ close to $\kappa = 3/5$ should behave similarly to the equal energy data and are expected to collapse.

In Fig. (5) we plot the analyticity strip width $\rho(\tau)$ as a function of τ for various values of κ, showing different kind of behaviors. For $\kappa = \{1/5, 4/5, 5/5\}$ $\rho(\tau)$ develops oscillations and never reach zero. These initial conditions are not exactly periodic as

[8] Since $\text{Arg}[\alpha_n] = B_n \in (-\pi, \pi)$ we first *unwrap* the phases before plotting the actual values. This amounts to shift $B_n \to B_n + 2\pi k$, $k \in \mathbb{Z}$ every time that $\Delta B_n = B_{n+1} - B_n$ changes sign.

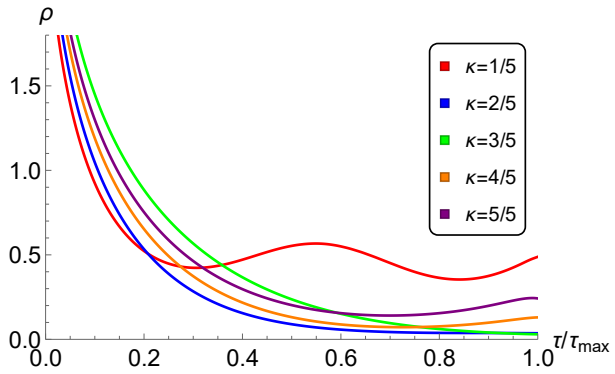

Figure 5: The evolution of the analyticity strip width $\rho(\tau)$, for different ratios of the energy in the first two modes.

the single–mode solutions but exibith revivals at time scales of order $1/\epsilon^2$ [37, 38]. For $\kappa = 2/5$ we do not see oscillations before $\tau_{\rm max}$ but by doing the fit we find that ρ_∞ is marginally above $1/n_{\rm max}$. We conjecture that this case is close to the borderline of a subspace of solutions that collapse at infinite τ, which for the two-mode initial data (3.1) is given by an open set with $\kappa \in (\kappa_{\rm min}, \kappa_{\rm max})$. We further studied the phase spectrum of all these initial data, and found always good agreement with the coherent phase ansatz.

3.2 A speed limit for energy transfer

It is interesting and surprising that some initial data appears to cascade to arbitrarily high frequencies in finite time, while other initial conditions take an infinite time. To really convince ourselves that the energy cascade takes infinite slow time for some initial conditions, we need an analytic argument. In this section, we give a simple argument showing that for solutions where two low modes dominate the spectrum, the remaining modes obey a simple speed limit in how fast energy can propagate to high frequencies. Our result rests on a strong assumptions that the solution is dominated by two low modes, and it would be very interesting to relax this assumption.

For this purpose it is convenient to write the equations of motion for the truncated resonant system in terms of complex amplitudes $\alpha_n \equiv A_n \exp(iB_n)$. The equations of motion become

$$2i\omega_n \frac{d\alpha_n}{d\tau} = \sum_{i+j=k+n} C_{ijkn}\alpha_i\alpha_j\bar{\alpha}_k \tag{3.4}$$

Now we will assume that the solution is dominated by two low modes; for definiteness, take modes $n = 0, 1$, but the basic structure of our results will remain unchanged. In

this case, we can keep only terms in the sum where two of the indices take the values $0, 1$. Since we have to obey the resonance condition $i + j = k + n$, for $n > 2$ this means that $k = 0, 1$, leaving the equation

$$2i\omega_n \frac{d\alpha_n}{d\tau} = 2C_{1(n-1)0n}\ \alpha_1\alpha_{n-1}\bar{\alpha}_0 + 2C_{0n0n}\alpha_0\alpha_n\bar{\alpha}_0 + 2C_{1n1n}\alpha_1\alpha_n\bar{\alpha}_1 + 2C_{0(n+1)1n}\alpha_0\alpha_{n+1}\bar{\alpha}_1 \tag{3.5}$$

Collecting terms and using the symmetries of the C coefficients, we get

$$i\omega_n \frac{d\alpha_n}{d\tau} - (C_{0n0n}\alpha_0\bar{\alpha}_0 + C_{1n1n}\alpha_1\bar{\alpha}_1)\,\alpha_n = C_{1(n-1)0n}\ \alpha_1\bar{\alpha}_0\alpha_{n-1} + C_{1n0(n+1)}\alpha_0\bar{\alpha}_1\alpha_{n+1} \tag{3.6}$$

Despite the complicated coefficients, this equation has two simplifying features:

- It is linear in the amplitudes α_n.
- It is *local*: a given mode is only influenced by its nearest neighbors (in addition to modes 0 and 1, which we think of as a background.)

We are interested in large mode numbers n. Since the C coefficients are smooth functions, and n is large, we take $C_{1n0(n+1)} \approx C_{1(n-1)0n} \equiv C_n$. We treat the dominant modes $\alpha_{0,1}$ as constants (it would be interesting to allow for time dependence).

As discussed above, the overall phase and the relative phase between any *two* modes is unphysical, so we are free to choose convenient phases for $\alpha_{0,1}$. We use this freedom to take the product $\alpha_0\bar{\alpha}_1$ to be pure imaginary for convenience, leading to the equation

$$i\omega_n \frac{d\alpha_n}{d\tau} - \left(C_{0n0n}A_0^2 + C_{1n1n}A_1^2\right)\alpha_n = iC_{1(n-1)0n}\ A_1A_0(\alpha_{n-1} - \alpha_{n+1}) \tag{3.7}$$

This equation can be written in the simpler notation

$$\frac{d\alpha_n}{d\tau} + id_n\alpha_n + \frac{1}{2}c_n(\alpha_{n+1} - \alpha_{n-1}) = 0 \tag{3.8}$$

with the definitions

$$d_n \equiv \frac{C_{0n0n}A_0^2 + C_{1n1n}A_1^2}{\omega_n} \qquad\qquad c_n \equiv \frac{2C_{1(n-1)0n}\ A_1A_0}{\omega_n} \tag{3.9}$$

Since a given mode couples to nearest neighbors, we would like to identify the speed at which signals can propagate in frequency space. To estimate this, take a continuum limit of the above equation, treating n as a continuous variable, to get

$$\frac{\partial\alpha}{\partial\tau} + id_n\alpha + c_n\frac{\partial\alpha}{\partial n} = 0 \tag{3.10}$$

We have not fully analyzed this equation, but the speed of propagation can be read off by comparing the coefficient of the time derivative to the space derivative, yielding a speed of propagation that depends on the mode number

$$\text{speed} = \frac{dn}{d\tau} = c_n \tag{3.11}$$

It is now interesting to ask whether energy can propagate to arbitrarily large mode numbers in finite time. The time to reach infinitely large mode numbers is

$$\Delta\tau = \int^{\infty} \frac{dn}{c_n} \tag{3.12}$$

Whether this is infinite depends on the function c_n, which depends on the dimension. In all dimensions, $\omega_n \sim n$. In 3+1 dimensions, the interaction coefficient $C_{1(n-1)0n} \sim n^2$ [14, 15]. Therefore, in 3+1 dimensions, $c_n \sim n$, and the integral is logarithmically divergent, and the cascade cannot reach infinity in finite time. The maximum excited mode number as a function of time can increase at most as $n_{\max} \sim \exp(a\tau)$. This agrees well with the observation in our numerical evolution that the spectrum has an exponential form $\exp(-\rho n)$ with $\rho \sim \exp(-a\tau)$.

In higher than 3+1 bulk dimensions, we expect the interaction coefficients to scale with larger powers of n, leading to a scaling $c_n \sim n^p$ with $p > 1$. This renders the integral convergent, meaning that energy can reach infinite mode number in finite time. This is in good agreement with the results obtained in [31] in 4+1 dimensions, where the spectrum was observed to approach a power law in finite time.

As a reminder, we were able to reach this strong conclusion by making a strong assumption that modes 0 and 1 dominate throughout the evolution. We expect a similar result whenever we assume that the evolution is dominated by a finite number of low-frequency modes: the equation for the high modes will still become linear and quasi-local, with the degree of nonlocality in frequency space determined by the frequency of the low modes that are excited.

On the other hand, the assumption that the solution is dominated by a few low modes can clearly break down as energy is transferred to higher modes. For this reason, it is not at all clear that the 'speed limit' found under this assumption is a robust result, although it is intriguing that it appears to agree with numerical results. It would be very interesting to derive a more generally valid speed limit on the rate of energy transfer.

4. Gaussian Data

In this section we study scalar fields with Gaussian profiles of the form $\phi(0, x) = 2\exp\left(-\frac{\tan^2 x}{\sigma^2}\right)$ in TTF where previous simulations, in the full GR system, reported that the collapse

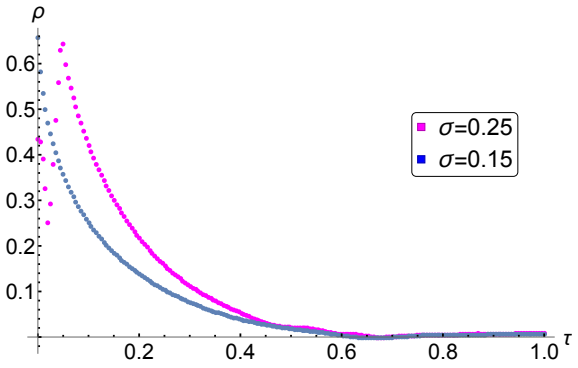

Figure 6: The evolution of the analyticity strip width $\rho(\tau)$ for Gaussian data with $\sigma = 0.25$ and $\sigma = 0.15$. In both case ρ becomes zero in finite slow time $\tau_\star \sim 0.625$.

depends on the width of profile [6,39]. We concentrate our study on profiles with widths $\sigma < 0.3$. We present results for two cases, with $\sigma = 0.15$ and $\sigma = 0.25$. We follow the same analysis as the one of Sec.(3), so we will not repeat the details here. One thing we would like to mention is that here the case is more clear since these initial approach a power-law spectrum in finite time and therefore we only use the truncation of $n_{max} = 200$. One other thing is that now we have $\tau_{max} = \tau_\star$, namely, we trust the evolution up to the time of the collapse $\tau_\star$.

In Fig (6) we plot the evolution of the analyticity strip width, for the two above-mentioned data to make precise the contrast with the 2–mode data. Here $\rho(\tau)$ goes to zero in **finite slow time** $\tau_\star \sim 0.625$. Our results agree with the observation of [6], that collapse happens for narrow profiles ($\sigma < 0.3$), but disagree with [35] on the resulting power-law of the energy cascade. We find that by the time of the collapse, or equivalently when the analyticity strip width $\rho(\tau)$ goes to zero, the power $\gamma(\tau)$ approaches a value very close to 3/2 and not 8/5.

In Fig.(7) and Fig.(8) we present the evolution of the amplitude spectra for Gaussian initial data with $\sigma = 0.15$ and $\sigma = 0.25$ respectively, towards a power law and we contrast the two above-mentioned values. We see that indeed the value $\gamma(\tau_\star) = 3/2$ is a better fit. We would like to mention at this point that the numerics are very subtle in AdS_4 and although our results strongly suggest a power law of 3/2, another value for γ very close to this one is still a possibility.

To illustrate the subtleties of the numerical methods we now study into more detail the fitting methods for the case of the $\sigma = 0.15$ Gaussian data close to the *collapse* point $\tau_\star \sim 0.625$. We fit the data in the range $30 \leq n \leq 110$ in order to to take into account only the asymptotic form of the spectrum and avoid cut-off effects. In Table 1

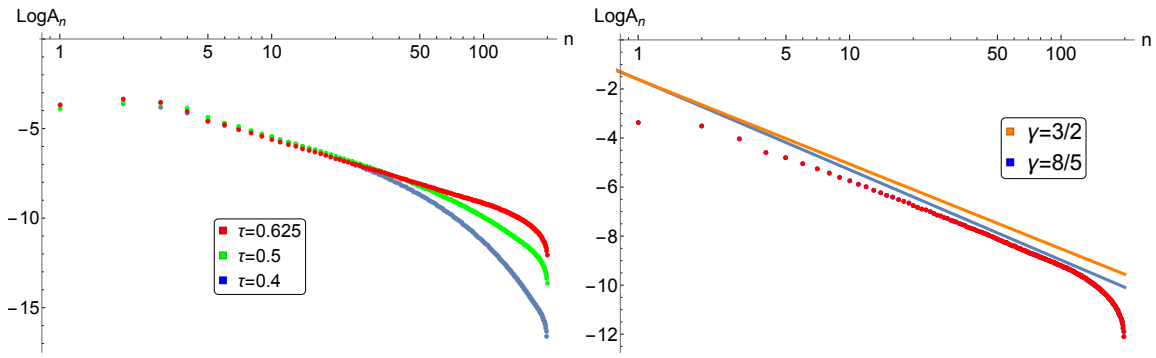

Figure 7: Left: The evolution of the amplitude spectra for Gaussian data with $\sigma = 0.15$ towards a power law $\gamma(0.625) \sim 3/2$ in the TTF system. **Right**: Comparison of the two power-laws with the actual data at the time of *collapse*, $\tau_\star = 0.625$.

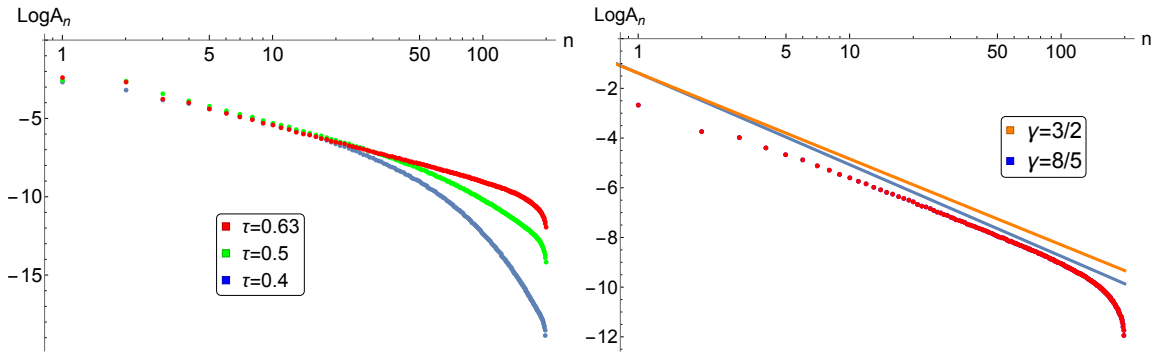

Figure 8: Left: The evolution of the amplitude spectra for Gaussian data with $\sigma = 0.25$ towards a power law $\gamma(0.63) \sim 3/2$ in the TTF system. The evolution is almost identical to the case of $\sigma = 0.15$. **Right**: Comparison of the two power-laws with the actual data at the time of *collapse*, $\tau_\star \sim 0.63$.

we present the fitting functions for three different values of $\tau = \{0.62, 0.625, 0.63\}$ and we fit both a power law spectrum and a power law spectrum with an exponential decay. We observe that the analyticity strip width turns from positive, at $\tau = 0.625$ to negative, at $\tau = 0.63$ which means that it hits zero in finite slow time. Also, at $\tau = 0.625$ it has the smallest value, and we believe that this is the most relevant time. However we don't have exact data for which $\rho = 0$. Two things that we would like to notice here is that although the value of the exponent is very small, it plays a significant role in estimating the exact value of the power γ and that the exact range of data that we use for the fitting affect the result as well[9]. The fits, in both cases suggest a power

[9]We chose the above-mentioned range, $n \in [30, 110]$, since it represents the most linear part of the

	$\tau = 0.62$		$\tau = 0.625$		$\tau = 0.63$	
	Parameter	*Error*	*Parameter*	*Error*	*Parameter*	*Error*
$\mathbf{A_n \sim \alpha n^{-\gamma} e^{-\rho n}}$						
$\mathrm{Log}(\alpha)$	-2.17944	0.02399	-2.18595	0.0301	-2.20568	0.03769
γ	1.51033	0.0077	1.51579	0.00966	1.517	0.012
ρ	0.000754	0.00012	0.000205	0.000151	0.000272	0.000189
$\mathbf{A_n \sim \alpha n^{-\gamma}}$						
$\mathrm{Log}(\alpha)$	-2.03288	0.00649	-2.14604	0.00672	-2.25847	0.00843
γ	1.55796	0.00154	1.52876	0.0016	1.49985	0.002

Table 1: The fitting values and the corresponding errors for three different times very close to the collapse time $\tau_\star \sim 0.625$, in the case of a power law with an exponential (**up**) and a power law alone (**down**).

law very close to 3/2, however as we mentioned earlier, values close to this one are also possible.

In Fig.(9) we present again the phase-spectrum as a function of the mode number n for different slow times. As we did earlier, we *unwrap* the phases, and we fit the data in the range[10] $60 \leq n < 140$ to a linear function and we quantify the deviation from linearity by subtracting the fitting value from the actual data. We see once more that the linear fit is a very good approximation, however interesting patterns appear, especially for late times, that might suggest towards a slight improvement to the perfectly coherent spectrum. We hope we will come back to this issue in a future work.

5. Conclusion

In this work we presented strong evidence that the turbulent cascade of energy towards modes of higher frequency in the problem of the instability of global AdS, happens in a *phase–coherent* way, as it was initially conjectured in [5]. Our results however leave room for possible small improvements on this idea and we believe it is something worth looking at in the future. On top of that, the perturbations that we studied here are also initially phase coherent and one might think that this could play a role in the later-time coherence of the phases. A natural generalization would be to study the development of phase coherence in perturbations that are not initially phase coherent[11].

plot and neglects the cut-off effect.

[10] As usual, we do so in order to address the *large n limit* and to avoid cut-off effects.

[11] We will come back to this issue in future work, but some preliminary results that we have suggest

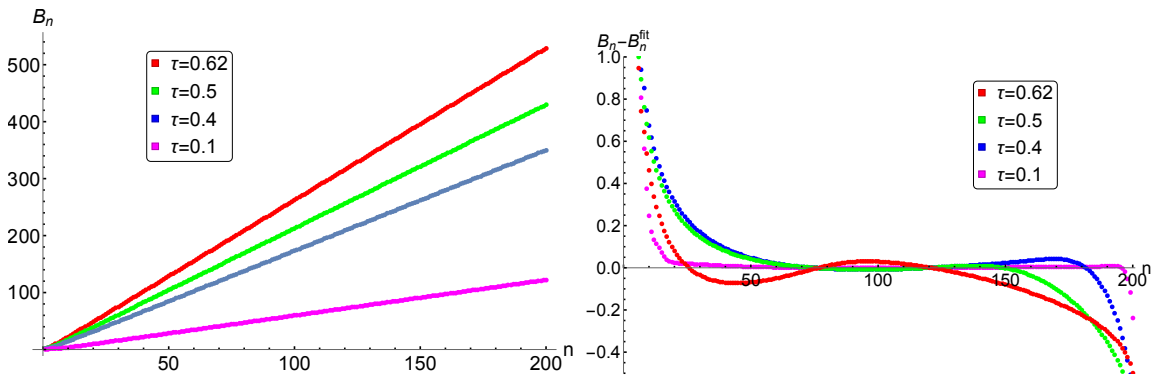

Figure 9: Left: The phases of the modes as a function of the mode number n when *unwraped* for different slow times τ. **Right:** The difference between the fitted and actual values as a function of n.

We have also studied the evolution of the amplitude spectra for the controversial two mode data and our work, combining numerical and analytical results, suggests that the collapse will happen in infinite slow time $\tau_\star \to \infty$. For the Gaussian initial data with $\sigma < 0.3$ we observed that the spectrum if the amplitudes approaches a power-law at finite slow time $\tau_\star \sim 0.625$, and the results suggest the power at the time of the collapse being very close to $\gamma(\tau_\star) \sim 3/2$. It would be very interesting to determine the power-law in the case of the two mode data and see if it agrees with the above-mentioned value, as well as to obtain a definite answer for the precise value in the case of the Gaussian data, perhaps through analytic techniques.

Acknowledgments

We thank I-Sheng Yang, Joanna Jalmuzna, Javier Mas, Oscar Dias, Jorge Santos, Andrzej Rostworowski and Antonio Rotundo for useful discussions. This work is part of the Δ-ITP consortium and also supported in part by the Foundation for Fundamental Research on Matter (FOM), both are parts of the Netherlands Organisation for Scientific Research (NWO) that is funded by the Dutch Ministry of Education, Culture and Science (OCW). FD is supported by GRAPPA PhD Fellowship. The research of JFP is supported by the Netherlands Organization for Scientific Research (NWO) under the VENI scheme.

that even in data for which the phases are initially randomly distributed, the higher modes are excited coherently

References

[1] P. Bizon and A. Rostworowski, "On weakly turbulent instability of anti-de Sitter space," *Phys.Rev.Lett.* **107** (2011) 031102, arXiv:1104.3702 [gr-qc].

[2] F. V. Dimitrakopoulos, B. Freivogel, J. F. Pedraza, and I.-S. Yang, "Gauge dependence of the AdS instability problem," *Phys. Rev. D* **94** (December, 2016) 124008, arXiv:1607.08094 [hep-th].

[3] F. Dimitrakopoulos and I.-S. Yang, "Conditionally Extended Validity of Perturbation Theory: Persistence of AdS Stability Islands," *Phys. Rev. D* **92** (2015) no. 08, 083013, arXiv:1507.02684 [hep-th].

[4] F. V. Dimitrakopoulos, B. Freivogel, M. Lippert, and I.-S. Yang, "Position space analysis of the AdS (in)stability problem ," *JHEP* (2015) , arXiv:1410.1880 [hep-th].

[5] B. Freivogel and I.-S. Yang, "Coherent Cascade Conjecture for Collapsing Solutions in Global AdS," *Phys. Rev. D* **93** (2016) 103007, hep-th/1512.04383.

[6] A. Buchel, S. L. Liebling, and L. Lehner, "Boson stars in AdS spacetime," *Phys.Rev.* **D87** (2013) no.˜12, 123006, arXiv:1304.4166 [gr-qc].

[7] S. R. Green, A. Maillard, L. Lehner, and S. L. Liebling, "Islands of stability and recurrence times in AdS," *Phys. Rev.* **D92** (2015) no.˜8, 084001, arXiv:1507.08261 [gr-qc].

[8] M. Maliborski and A. Rostworowski, "Time-Periodic Solutions in an Einstein AdS–Massless-Scalar-Field System," *Phys.Rev.Lett.* **111** (2013) no.˜5, 051102, arXiv:1303.3186 [gr-qc].

[9] N. Deppe and A. R. Frey, "Classes of Stable Initial Data for Massless and Massive Scalars in Anti-de Sitter Spacetime," *JHEP* (December, 2015) , arXiv:1508.02709 [hep-th].

[10] G. T. Horowitz and J. E. Santos, "Geons and the Instability of Anti-de Sitter Spacetime," arXiv:1408.5906 [gr-qc].

[11] O. J. Dias and J. E. Santos, "AdS nonlinear instability: moving beyond spherical symmetry," arXiv:1602.03890 [hep-th].

[12] A. Rostworowski, "Comment on "AdS nonlinear instability: moving beyond spherical symmetry"," arXiv:1612.00042 [hep-th].

[13] V. Balasubramanian, A. Buchel, S. R. Green, L. Lehner, and S. L. Liebling, "Holographic Thermalization, Stability of AdS, and the FPU Paradox," arXiv:1403.6471 [hep-th].

[14] B. Craps, O. Evnin, P. Jai-akson, and J. Vanhoof, "Ultraviolet asymptotics for quasiperiodic AdS_4 perturbations," *JHEP* **10** (2015) 080, arXiv:1508.05474 [gr-qc].

[15] B. Craps, O. Evnin, and J. Vanhoof, "Ultraviolet asymptotics and singular dynamics of AdS perturbations," *JHEP* **10** (2015) 079, arXiv:1508.04943 [gr-qc].

[16] B. Craps, O. Evnin, and J. Vanhoof, "Renormalization group, secular term resummation and AdS (in)stability," arXiv:1407.6273 [gr-qc].

[17] B. Craps, O. Evnin, and J. Vanhoof, "Renormalization, averaging, conservation laws and AdS (in)stability," arXiv:1412.3249 [gr-qc].

[18] O. J. C. Dias, J. E. Santos, and B. Way, "Numerical Methods for Finding Stationary Gravitational Solutions," *Class. Quant. Grav.* **33** (2016) no.˜13, 133001, arXiv:1510.02804 [hep-th].

[19] O. J. Dias, G. T. Horowitz, D. Marolf, and J. E. Santos, "On the Nonlinear Stability of Asymptotically Anti-de Sitter Solutions," *Class.Quant.Grav.* **29** (2012) 235019, arXiv:1208.5772 [gr-qc].

[20] O. J. Dias, G. T. Horowitz, and J. E. Santos, "Gravitational Turbulent Instability of Anti-de Sitter Space," *Class.Quant.Grav.* **29** (2012) 194002, arXiv:1109.1825 [hep-th].

[21] N. Deppe, "On the stability of anti-de Sitter spacetime," arXiv:1606.02712 [gr-qc].

[22] J. Abajo-Arrastia, E. da Silva, E. Lopez, J. Mas, and A. Serantes, "Holographic Relaxation of Finite Size Isolated Quantum Systems," *JHEP* **1405** (2014) 126, arXiv:1403.2632 [hep-th].

[23] J. Mas and A. Serantes, "Oscillating Shells in Anti-de Sitter Space," *Int. J. Mod. Phys. D* **24** (2015) no.˜09, , arXiv:1507.01533 [gr-qc].

[24] I.-S. Yang, "Missing top of the AdS resonance structure," *Phys.Rev.* **D91** (2015) no.˜6, 065011, arXiv:1501.00998 [hep-th].

[25] V. Cardoso and J. V. Rocha, "Collapsing shells, critical phenomena and black hole formation," *Phys. Rev. D* **93** (2016) no.˜8, , arXiv:1601.07552 [gr-qc].

[26] D. S. Olivan and C. F. Sopuerta, "Moving Closer to the Collapse of a Massless Scalar Field in Spherically Symmetric Anti-de Sitter Spacetimes," 1603.03613.

[27] N. Jokela, A. Ponni, and A. Vuorinen, "Small black holes in global AdS spacetime," *Phys. Rev. D* **93** (2016) no.˜08, 086004, arXiv:1508.00859.

[28] K. Hashimoto, M. Nishida, and A. Sonoda, "Universal turbulence on branes in holography," *JHEP* (August, 2015) , arXiv:1504.07836 [hep-th].

[29] P. Basu, C. Krishnan, and P. Bala Subramanian, "AdS (In)stability: Lessons From The Scalar Field," *Phys.Lett.* **B746** (2015) 261–265, arXiv:1501.07499 [hep-th].

[30] P. Basu, C. Krishnan, and A. Saurabh, "A Stochasticity Threshold in Holography and and the Instability of AdS," arXiv:1408.0624 [hep-th].

[31] P. Bizon, M. Maliborski, and A. Rostworowski, "Resonant dynamics and the instability of anti-de Sitter spacetime," arXiv:1506.03519 [gr-qc].

[32] C. Sulem, P.-L. Sulem, and F. Helene, "Tracing complex singularities with spectral methods," *J. Comput. Phys.* **50** (1983) 138.

[33] P. Bizon and J. Jalmuzna, "Globally regular instability of AdS_3," *Phys.Rev.Lett.* **111** (2013) no.˜4, 041102, arXiv:1306.0317 [gr-qc].

[34] P. Bizon and A. Rostworowski, "Comment on "Holographic Thermalization, stability of AdS, and the Fermi-Pasta-Ulam-Tsingou paradox" by V. Balasubramanian et al," arXiv:1410.2631 [gr-qc].

[35] M. Maliborski and A. Rostworowski, "Lecture Notes on Turbulent Instability of Anti-de Sitter Spacetime," *Int.J.Mod.Phys.* **A28** (2013) 1340020, arXiv:1308.1235 [gr-qc].

[36] A. Buchel, S. R. Green, L. Lehner, and S. L. Liebling, "Reply to "Comment on two-mode stability islands around AdS"," arXiv:1506.07907 [gr-qc].

[37] J. Abajo-Arrastia, E. da Silva, E. Lopez, J. Mas, and A. Serantes, "Holographic Relaxation of Finite Size Isolated Quantum Systems," *JHEP* **05** (2014) 126, arXiv:1403.2632 [hep-th].

[38] E. da Silva, E. Lopez, J. Mas, and A. Serantes, "Collapse and Revival in Holographic Quenches," *JHEP* **04** (2015) 038, arXiv:1412.6002 [hep-th].

[39] M. Maliborski and A. Rostworowski, "A comment on "Boson stars in AdS"," arXiv:1307.2875 [gr-qc].